Modeling Dynamic Dilemma Zones and its Applications

A Paper Submitted to
Ohio Transportation Consortium
for the 2009 OTC Student Paper Competition

By

Zhixia Li
PhD Student in Transportation Engineering
Art-Engines Transportation Lab, 735 Engineering Research Center
Department of Civil and Environmental Engineering
University of Cincinnati, College of Engineering
Cincinnati, Ohio 45221-0071
Tel: (513) 484-2991; E-mail: lizx@email.uc.edu

Total words: 4876 (not including references, tables, and graphics)

ABSTRACT

Dilemma zone is dynamically featured both in location and length at high speed signalized intersections due to varying driving behaviors in response to yellow indications. Constant contributing factors are traditionally used to compute a dilemma zone, and it is hard to reflect its dynamic characteristics, and arbitrary dilemma zone locations are possibly generated. To overcome this problem, this paper presents a novel approach for modeling dynamic dilemma zones, which identifies varying values of dilemma zone contributing factors, i.e. acceleration rate, deceleration rate and driver's perception reaction time, under different approaching speeds using observed vehicle trajectory data. A case study was conducted at a high speed intersection in Fairfield, Ohio. Time-based yellow-onset trajectories were obtained using video-capture-based technique and were then used to calibrate the dynamic dilemma zone model. Two alternative sets of ground-truth data considering different levels of driving aggressiveness were established for the model calibration. The calibrated model well reflects the real-world dynamic driving behaviors with varying values of contributing factors. As an application, dilemma zone lookup charts were developed based on the calibrated dynamic dilemma zone models. These charts provide a user-friendly tool for checking the location and length of a dilemma zone for a specific speed in response to a certain yellow duration. Another important contribution is the definition and modeling of the concept Dilemma Conflict Potential (DCP). It can quantitatively measure the dilemma hazard for each vehicle in terms of the probability of traffic conflict. Six scenarios are considered for describing the DCP, and each has its specific equation that models the DCP with vehicles' yellow-onset speed and position. DCP considers speed and location information when modeling the dilemma hazard, and is a more comprehensive measure than traditionally using the "number vehicles in dilemma zone". Significantly, the methodology used in this paper is capable of satisfying the needs of states in the U.S. for updating their local dilemma zone tables, and establishes a solid basis for developing the optimal dilemma zone protection strategies.

Modeling Dynamic Dilemma Zones and its Applications

Zhixia Li

INTRODUCTION

Among all possible factors contributing to the intersection-signal-related crashes, yellow interval dilemma is one of the major problems that have not been fully solved yet.

A dilemma zone (DZ) is a roadway segment within which a vehicle approaching an intersection during the yellow interval can neither safely clear the intersection, nor stop comfortably at the stop line (Gazis, 1960). It is formed due to the minimum safe stopping distance (X_c) being longer than the maximum yellow clearance distance (X_0), as illustrated by Figure 1.a.

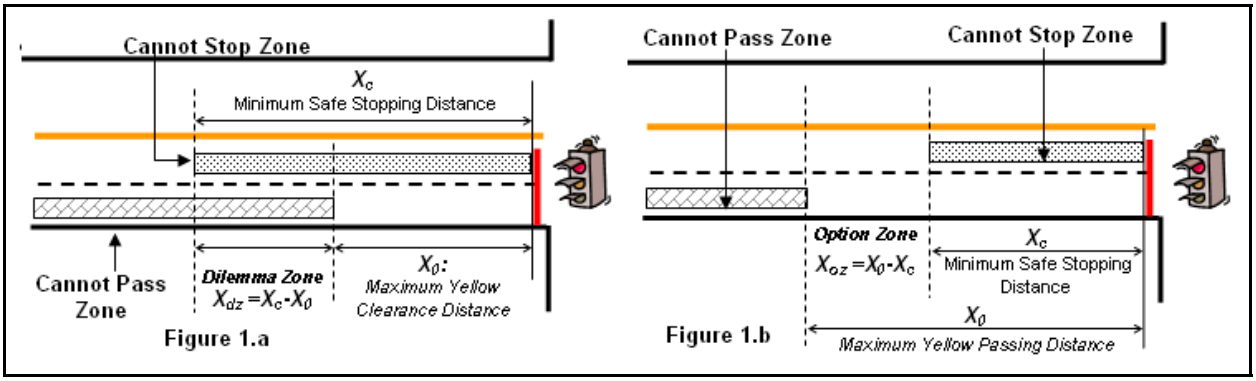

Figure 1. Formation of Dilemma Zone and Option Zone

This definition along with its mathematical model, i.e., the GHM model, is further applied in the ITE handbooks (ITE, 1982; 1999) as a guideline for determining the yellow change and all-red clearance intervals. Based on the "ITE yellow interval formula" and assumed parameter values (i.e. driver's perception-reaction time as 1.0s, and vehicle's deceleration rate as 10 ft/s^2), the calculated yellow time theoretically guarantees that X_0 is longer than X_c. Thus, it would be ensured for an approaching vehicle to either safely stop or clear the intersection during the yellow interval. At this point, the defined yellow dilemma is supposed not to exist. However, in reality this yellow dilemma is hard to be eliminated because: (1) drivers' driving behaviors vary with their different aggressiveness, and the assumed parameter values may not be compatible with all the possible driving features. In other words, DZ is dynamically featured in location and length (Moon and Coleman, 2002; Chang and Liu, 2006), and this dynamics is reflected by the varying values of dilemma zone contributing factors, i.e. perception-reaction time (PRT), acceleration rate for passing, and deceleration rate for stopping; and (2) even though when X_0 is longer than X_c, an option zone (OZ) is formed, as is illustrated by Figure 1.b. Drivers within the OZ at the yellow onset still experience indecisiveness (dilemma) about making pass or stop decisions, which also makes them highly exposed to rear-end or right-angle crashes (Saito et al., 1990; Koll et al., 2004).

Therefore, the yellow dilemma is understood as the result of existence of either DZ or OZ, and it cannot be actually eliminated. However, the effect caused by it can be reduced by applying advance loops detection and green extension strategies, which aim to clear all approaching vehicles out of DZ and OZ before the onset of yellow. In this way, an accurate DZ/OZ table is essential for correctly placing the advance loops. However, the locations of X_c and X_0 in the table

are used to be calculated using assumed and constant values of contributing factors based on infrastructure design experiences (FHWA, 2006; Pant et al., 2005). Such a calculation is unable to reflect the dynamics of both driving behaviors and the DZ/OZ, and then possibly yields inaccurate DZ/OZ locations. It is hence a challenge to increase accuracy and reliability of the DZ/OZ table in estimating the locations of dynamic DZs and OZs.

Recently, Chang and Liu (2006) used *fixed spatial-point* trajectory data to facilitate obtaining the locations of dynamic DZs. They calculated the DZ lengths based on the GHM model by using the average contributing factor values obtained from the trajectory data. It is a big advance in modeling the dynamic dilemma zones with trajectory data. But, calculating the DZ with those average observed factor values is still hard to reflect the DZ dynamics as well as the exact DZ locations.

This paper presents a new understanding and novel approach for modeling dynamic dilemma zones, which considers varying driving behavior factors with respect to different approaching speeds. The modeling is observation-based and can be calibrated using yellow-onset trajectory data. A high-speed signalized intersection in Cincinnati, Ohio is selected as the case study site for videotaping vehicles' reaction to the yellow indications. Video-capture-based software VEVID (Vehicle Video-Capture Data Collector) was developed to obtain high-resolution (up to 30 frames per second) *time-based* trajectory data at yellow onsets. *Time-based* trajectories enable obtaining the vehicles' speed and distance from stop line at the exact instant when the signal indication changes from green to yellow. Statistical analysis is performed on the yellow-onset trajectories to obtain two alternative sets of ground-truth data for calibrating the dynamic dilemma zone model at levels of different driving aggressiveness. As a result of calibration, the obtained values of contributing factors vary with vehicles' approaching speeds. It well reflects the nature of the dilemma zone dynamics. Finally, dilemma zone lookup charts are developed for practical use as a significant application of the calibrated dynamic dilemma zone model. And, the concept of Dilemma Conflict Potential (DCP) is proposed and theoretically modeled as an improved measurement of the dilemma hazard. DCP provides a solid basis for evaluating and developing advance loops layout for dilemma zone protection when used combined with the dilemma zone lookup table.

NEW UNDERSTANDING AND MODELING OF DYNAMIC DILEMMA ZONES

As discussed earlier, both OZ and DZ are actually two types of dilemma zones while they have different characteristics. DZ is viewed as a risky zone (RZ) that retains a hazardous chance for a vehicle happening to be located within this zone to run red, because the yellow duration is insufficient for the vehicle to safely pass the stop line while not sufficient distance for the vehicle to stop before the stop line. While not as risky as DZ, the OZ potentially causes the driver's hesitation in the decision-making process of deciding whether stop or pass. Therefore, the dilemma zone is defined in this paper as a general concept and it is composed of risky zone and option zone, which are referred to as DZ and OZ discussed in the previous section of the paper.

In the GHM model, the yellow interval is supposed to be used for clearing vehicles through the entire intersection (including the width of the intersection). However, based on field observations, when a driver perceives the yellow indication, he/she does not consider whether he/she could clear the intersection completely during the yellow interval. Actually, his/her concern is with whether he/she could pass the stop line before the onset of the red indication. Therefore, in this study, the intersection width and vehicle's length are not considered in

calculating the maximum yellow passing distance X_0. It is assumed that the yellow interval is only for clearing vehicles to the stop line rather than through the intersection.

Also, based on the results of previous studies, the values of the dilemma zone contributing factors are not constant but vary at different approaching speeds: the deceleration rate for stopping increases as the approaching speed increases (Gates et al., 2007; Moon et al, 2003); the acceleration rate for passing decreases as the approaching speed increases (Gazis, 1960); and the perception-reaction time of drivers decreases as the approaching speed increases (faster drivers reacts more quickly) (Gates et al., 2007).

Based on these understandings, the classic GHM model is modified as the following equations:

$$X_c(V_0) = V_0\delta_{stop}(V_0) + \frac{V_0^2}{2 \cdot a_{stop}(V_0)} \quad (1)$$

$$X_0(V_0) = V_0\tau + \frac{1}{2}a_{pass}(V_0) \cdot [\tau - \delta_{pass}(V_0)]^2 \quad (2)$$

Where, V_0 = vehicle's approaching speed (ft/s);
$X_c(V_0)$ = minimum stopping distance from the stop line at speed V_0 (ft);
$X_0(V_0)$ = maximum yellow passing distance from the stop line at speed V_0 (ft);
$\delta_{stop}(V_0)$ = driver's minimum PRT for safe stopping at speed V_0 (s);
$a_{stop}(V_0)$ = vehicle's maximum deceleration rate for safe stopping at speed V_0 (ft^2/s);
$\delta_{pass}(V_0)$ = driver's minimum PRT for safe passing at speed V_0 (s);
$a_{pass}(V_0)$ = vehicle's maximum acceleration rate for passing at speed V_0 (ft^2/s);
τ = duration of the yellow interval (s).

The length of the RZ can be modeled by Equation (3), when $X_c > X_0$, while the length of the OZ can be modeled by Equation (4), when $X_0 > X_c$.

$$L_{RZ}(V_0) = X_c(V_0) - X_0(V_0) = V_0\delta_{stop}(V_0) + \frac{V_0^2}{2 \cdot a_{stop}(V_0)} - \{V_0\tau + \frac{1}{2}a_{pass}(V_0) \cdot [\tau - \delta_{pass}(V_0)]^2\} \quad (3)$$

$$L_{OZ}(V_0) = X_0(V_0) - X_c(V_0) = V_0\tau + \frac{1}{2}a_{pass}(V_0) \cdot [\tau - \delta_{pass}(V_0)]^2 - [V_0\delta_{stop}(V_0) + \frac{V_0^2}{2 \cdot a_{stop}(V_0)}] \quad (4)$$

According to these equations, the locations of X_c and X_0 are highly related to the contributing factors: $\delta_{stop}(V_0)$, $a_{stop}(V_0)$, $\delta_{pass}(V_0)$, and $a_{pass}(V_0)$, while these factors are associated with the vehicle approaching speed V_0. However, the factors values that truly represent the real-world travel behaviors are greatly dependant upon field observations. An effective method is using the filed-observed $X_c(V_0)$s and $X_0(V_0)$s as ground-truth data to calibrate the X_c and X_0 models (Equations 1 and 2). In this way, the calibrated model with appropriate factor values can well represent the real-world dynamic driving behaviors. One obstacle for performing the model calibration is that the observed $X_c(V_0)$s and $X_0(V_0)$s cannot be directly obtained from the observation, even with the trajectory data. It is because the yellow-onset speeds and distances are dynamically distributed due to varying driving behaviors. Nevertheless, from the statistical point of view, profiles representing the relationship between the observed X_c

and V_0, and the relationship between the observed X_0 and V_0 can be simply obtained by performing regression analysis on the trajectory data. The results can provide appropriate ground-truth data for performing the model calibration.

To better present the new understanding and modeling of the dynamic dilemma zones using an observation-based approach, a heuristic framework illustrating the proposed concepts is developed as shown by Figure 2.

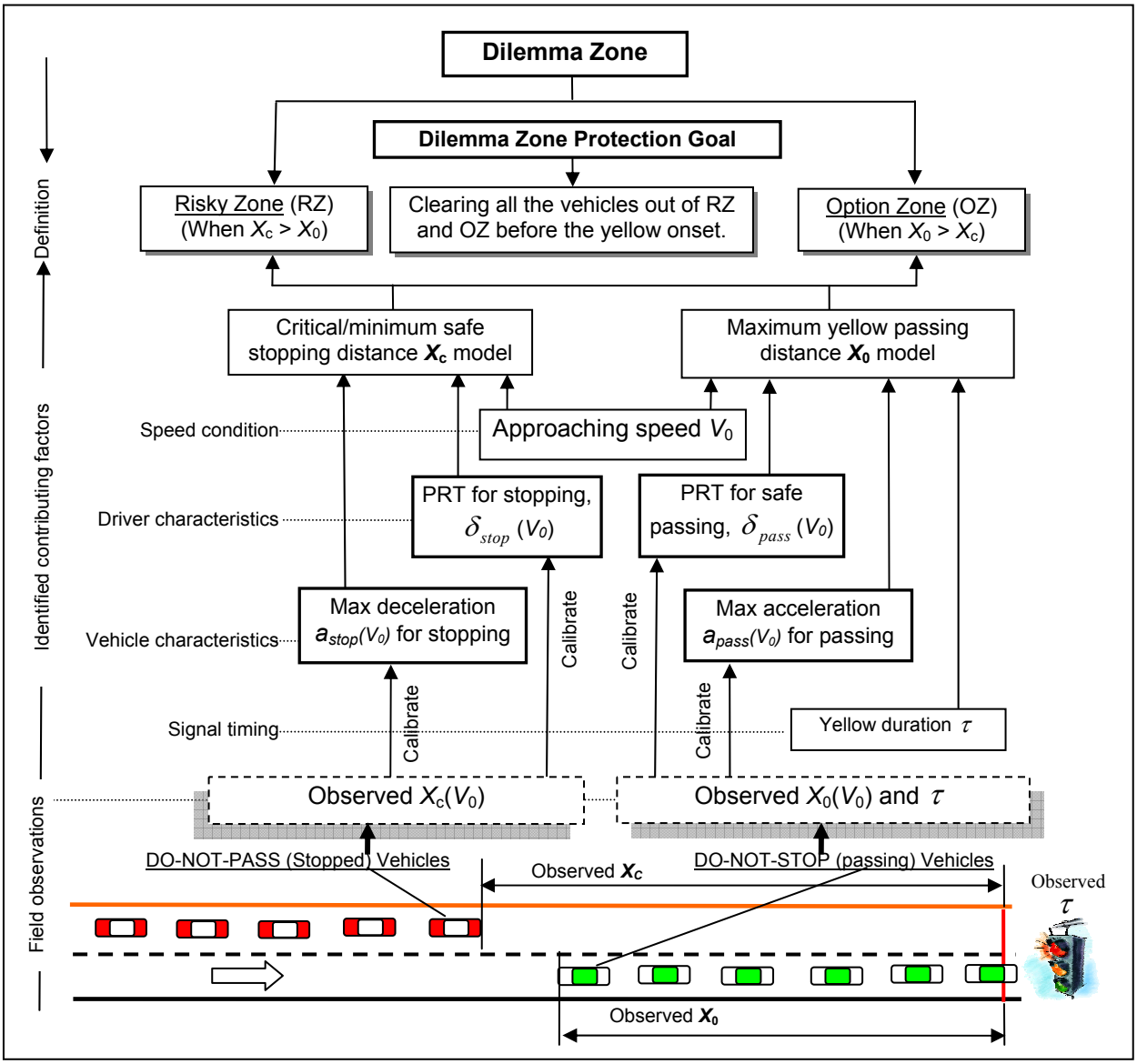

Figure 2. Heuristic Framework of Dynamic Dilemma Zone Modeling

DATA COLLECTION AND TRAJECTORY EXTRACTION

The intersection of OH-4 and Seward Rd, Fairfield, Ohio was selected as the case study site (see Figure 3), where the speed limit is 50 mph and the yellow interval is 4.5 seconds on the OH-4 approaches. In order to guarantee the full view coverage of the dilemma zone, two camcorders

were placed on the south side of the eastbound OH-4 at 300 and 500 ft from stop line, respectively. They were synchronized before videotaping, and 6.5-hour period of traffic operation was videotaped at this location.

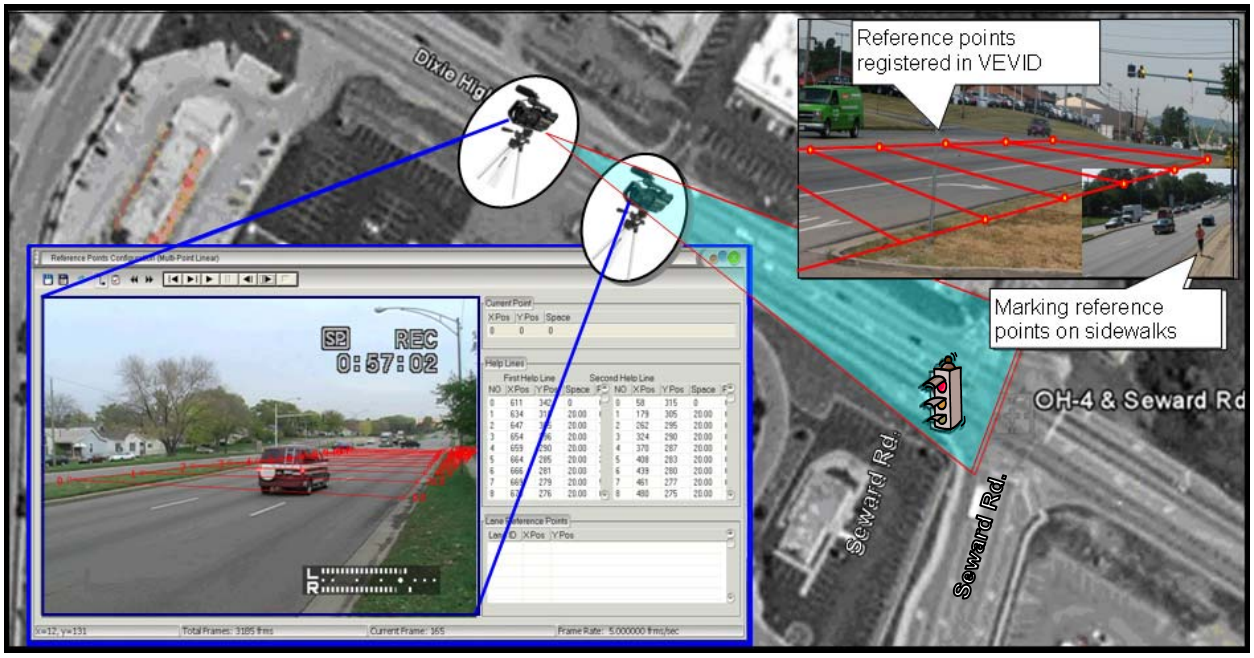

Figure 3. Video Data Collection and Trajectory Data Extraction

In field, reference points were set up from the stop line to the position of the camcorder at a fixed spacing of 20 ft along the curbs of both sides. They are used for VEVID to convert the screen-measured distance into the real world distance (Wei et al., 2005). A chalk was used to mark those points on the curbs, and then a surveyor stepped on each mark for a short while (e.g., 5 seconds). All these actions were recorded by the camcorder.

In office, the video was played back in the environment of VEVID. Then, the marked reference points were recognized and registered into the database of VEVID by identifying the surveyor's feet locations when he stepped on the marks in the video, as shown in the top-right corner of Figure 3. In VEVID, the videos can pause at each exact yellow onset, and real world yellow-onset distance from the targeted vehicle to the stop line can be obtained by simply clicking the mouse over the contacting point between the rear tire (or front tire) and the pavement. With the distance, the yellow onset speed can be derived by dividing the distance interval between the frame of yellow onset and the preceding frame by the time interval (e.g. the time interval between two consecutive frames at the frame rate of 30 fps is 1/30 second).

During each yellow interval, only the last-to-pass (excluding those run-reds) and the first-to-stop vehicle in each through lane were targeted for extracting the trajectory data, because only these vehicles directly contribute to the formation of dilemma zone.

Besides the yellow onset distance and speed, the acceleration rate for passing and the deceleration rate for stopping were also derived and recorded for each last-to-pass vehicle and first-to-stop vehicle. And, each driver's PRT for stopping was obtained and recorded through counting the number of frames elapsed from the yellow onset to the instant when the illumination of the brake light is observed. The time used by each last-to-pass vehicle to pass the stop line from the yellow onset was also recorded.

Totally, 522 qualified vehicle samples were obtained. As a result, the observed acceleration rate for passing ranges from -1.16 ft/s^2 to 13.03 ft/s^2; the observed deceleration rate for stopping ranges from -3.25 ft/s^2 to -16.1 ft/s^2; the observed PRT for stopping is within the range from 0.39 s to 2.12 s; and the observed time used to pass the stop line is within the range from 0.1 s to 4.5 s with the 95th percentile value being 4.23 s.

MODEL CALIBRATION WITH TRAJECTORY DATA

The model calibration is processed by trialing and fitting the modeled X_c and X_0 values (Based on Equations 1 and 2) to the ground-truth X_c and X_0 values, by seeking appropriate values of the contributing factors.

During the calibration, values of the contributing factors are guaranteed satisfying the following constrains: the deceleration rate for stopping increases as the approaching speed increases; the acceleration rate for passing decreases as the approaching speed increases; both PRTs for stopping and passing decrease as the approaching speed increases; and, all values of the contributing factors are within the observed ranges.

The dilemma zone model was calibrated using two different sets of ground-truth data representing different levels of driving aggressiveness.

Calibration Considering Extreme Driving Aggressiveness

The first set of ground-truth data is based on the observed maximum yellow passing distance and the observed minimum stopping distance, which represents the extreme driving aggressiveness. The model calibration process consists of the following steps.

Step 1: trajectories of the first-to-stop vehicles are plotted on a coordinate system with the yellow-onset speeds on the vertical axis and the yellow-onset distances from stop line on the horizontal axis, as is illustrated by Figure 4.

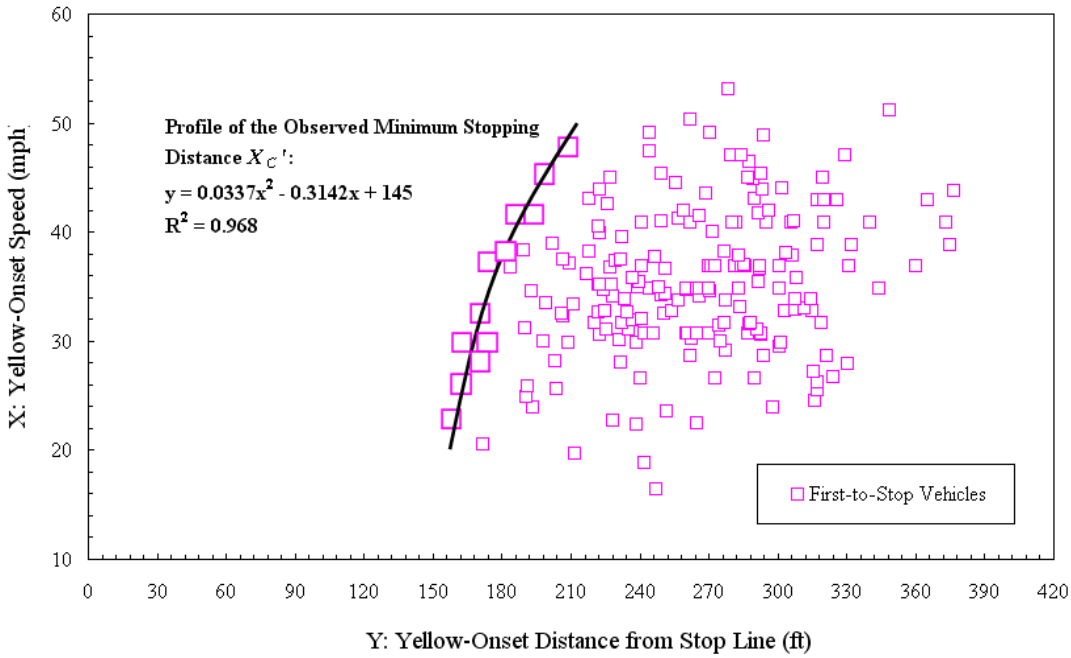

Figure 4. Identifying the Ground-truth Profile of the Observed Min Stopping Distance

The ground-truth profile of the observed minimum stopping distance X_c' is identified by performing regression analysis on those trajectories with minimum stopping distances at various speeds. The relationship between X_c' and V_0 can be expressed by the following equation.

$$X_c' = 0.0337V_0^2 - 0.3142V_0 + 145 \quad (5)$$
$$R^2 = 0.968$$

Step 2: Similarly, trajectories of the last-to-pass vehicles are also plotted on a coordinate system, as is illustrated by Figure 5.

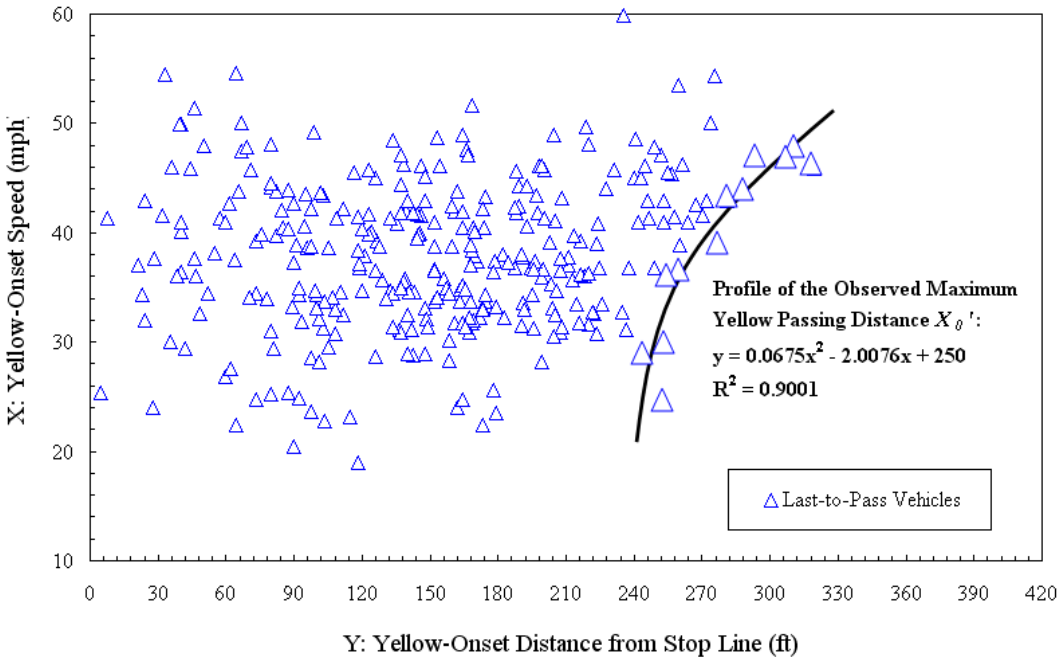

Figure 5. Identifying the Ground-truth Profile of the Max Yellow Passing Distance

The ground-truth profile of the observed maximum yellow passing distance X_0' is identified by performing regression analysis on those samples with maximum passing distances at various speeds. The relationship between X_0' and V_0 can be expressed by the following equation.

$$X_0' = 0.0675V_0^2 - 2.0076V_0 + 250 \quad (6)$$
$$R^2 = 0.9001$$

Step 3: With the ground-truth profiles of X_0' and X_c', a process of trial-and-fit method is then employed for calibrating the X_0 and X_c models. Appropriate values of the contributing factors are obtained through fitting the theoretically modelled X_c and X_0 values (based upon Equations 1 and 2) to the ground-truth X_0' and X_c' values (based upon Equations 5 and 6) at each given speed. The calibration process is illustrated by Figure 6.

The goodness-of-fit analysis shows that the correlation coefficient R^2 is 0.9998 between the profiles of X_c and X_c', while the number is 0.9997 between the profiles of X_0 and X_0'. Both R^2 values indicate a good fitting. Through the model calibration, appropriate values of $a_{stop}(V_0)$, $a_{pass}(V_0)$, $\delta_{pass}(V_0)$, and $\delta_{stop}(V_0)$ at various speeds are obtained and shown in Table 1. It has to

be noted that during the calibration of the X_0 model, the "time used by vehicles to pass the stop line (τ')" is set to 4.5 s, which is equal to the full yellow duration. It is because all these vehicles with observed maximum passing distances actually used up the entire yellow duration to pass the stop line (almost passing at the red-onset).

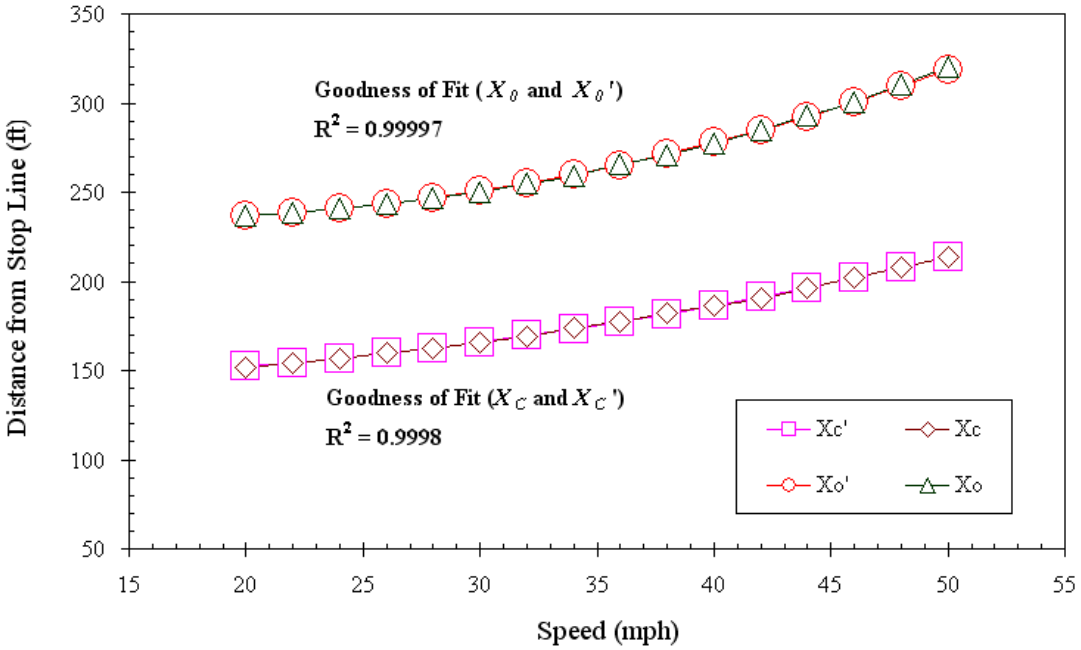

Figure 6. Process of the Model Calibration (Based on Ground-truth Data Set 1)

Table 1. Calibrated Values of Contributing Factors (Based on Ground-truth Data Set 1)

V_0 (mph)	τ' (s)	$\delta_{stop}(V_0)$ (s)	$a_{stop}(V_0)$ (ft/s^2)	$\delta_{pass}(V_0)$ (s)	$a_{pass}(V_0)$ (ft/s^2)	X_c (ft)	X_c' (ft)	X_0 (ft)	X_0' (ft)
20	4.5	0.6	-3.2	0.45	12.78	152	152	237	237
22	4.5	0.595	-3.86	0.425	11.21	154	154	238	239
24	4.5	0.59	-4.55	0.4	9.82	157	157	241	241
26	4.5	0.585	-5.28	0.375	8.48	160	160	244	243
28	4.5	0.58	-6.09	0.35	7.21	162	163	247	247
30	4.5	0.575	-6.89	0.325	5.98	166	166	250	251
32	4.5	0.57	-7.72	0.3	4.92	169	169	255	255
34	4.5	0.565	-8.54	0.275	3.92	174	173	259	260
36	4.5	0.56	-9.45	0.25	3.11	177	177	266	265
38	4.5	0.555	-10.29	0.225	2.21	182	182	271	271
40	4.5	0.55	-11.18	0.2	1.48	186	186	278	278
42	4.5	0.545	-12.07	0.175	0.78	191	191	284	285
44	4.5	0.54	-12.91	0.15	0.23	196	196	293	292
46	4.5	0.535	-13.72	0.1	-0.34	202	202	300	300
48	4.5	0.53	-14.55	0.05	-0.64	208	208	310	309
50	4.5	0.525	-15.35	0	-0.98	214	214	320	318

Calibration Excluding Extreme Driving Aggressiveness

The contributing factors calibrated by the first set of ground-truth data reflect the extreme conditions of driving behaviors, which usually yield long dilemma zones. From engineering viewpoints, those extremely conservative or aggressive driving behaviors need to be precluded from the ground-truth data by using x^{th} percentile observed passing distance (x^{th} percentile X_0') and $(1\text{-}x)^{th}$ percentile observed stopping distance [$(1\text{-}x)^{th}$ percentile X_c'] as the ground-truth data. And, the corresponding dilemma zone model is termed as the X^{th} Percentile Dilemma Zone.

Therefore, the second set of ground-truth data is based on the 95^{th} percentile X_0' and the 5^{th} percentile X_c', the dilemma zone model calibrated by which will refer to as the 95^{th} percentile dilemma zone. The entire model calibration process consists of the following steps.

Step 1: trajectories of the first-to-stop vehicles and last-to-pass vehicles are plotted on a coordinate system with the yellow-onset speeds on the vertical axis and the yellow-onset distances from stop line on the horizontal axis. All the trajectories are classified into 6 speed groups, which are 20-25 mph, 25-30 mph, 30-35 mph, 35-40 mph, 40-45 mph, and 45-50 mph, respectively.

Step 2: identify the 95^{th} percentile X_0' and the 5^{th} percentile X_c' for each speed group from the cumulative curves of the passing distance and stopping distance, respectively. Boundaries of the highlighted rectangles in Figure 7 represent the identified 5^{th} percentile X_c' and the 95^{th} percentile X_0' for each speed group. As illustrated in Figure 7, those circled stopped and passing vehicles are the precluded extremely conservative and aggressive drivers.

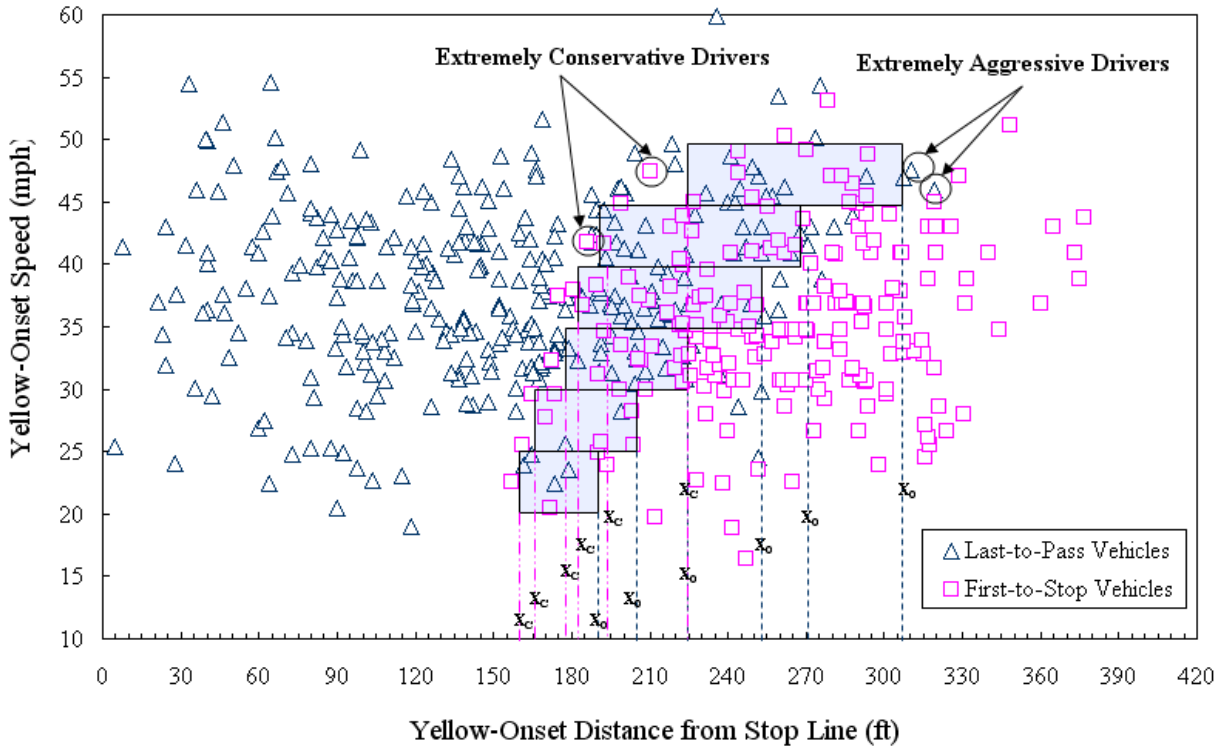

Figure 7. Identified 5^{th} Percentile X_c' and 95^{th} Percentile X_0' for Each Speed Group

Note that, for determining the 5^{th} percentile X_c' for each speed group, only those stopping distances shorter than the furthest passing distance within the speed group constitute the sample.

Step 3: use the mid-point speed of each speed group (e.g. use 37.5 mph for the speed group 35-40 mph) as the independent variable x, and the corresponding 5th percentile X_c' and 95th percentile X_0' as the dependant variables y, and perform the regression analysis. As is illustrated by Figure 8, profiles of the 5th percentile X_c' and the 95th percentile X_0' are identified. The relationship between the 5th percentile X_c' and V_0, and the relationship between the 95th percentile X_0' and V_0 can be mathematically expressed by the following equations, respectively.

$$X'_{C-5th} = 0.0553V_0^2 - 1.4247V_0 + 162 \quad (7)$$

$$R^2 = 0.9593$$

$$X'_{0-95th} = 0.0686V_0^2 - 0.1886V_0 + 159.1 \quad (8)$$

$$R^2 = 0.9957$$

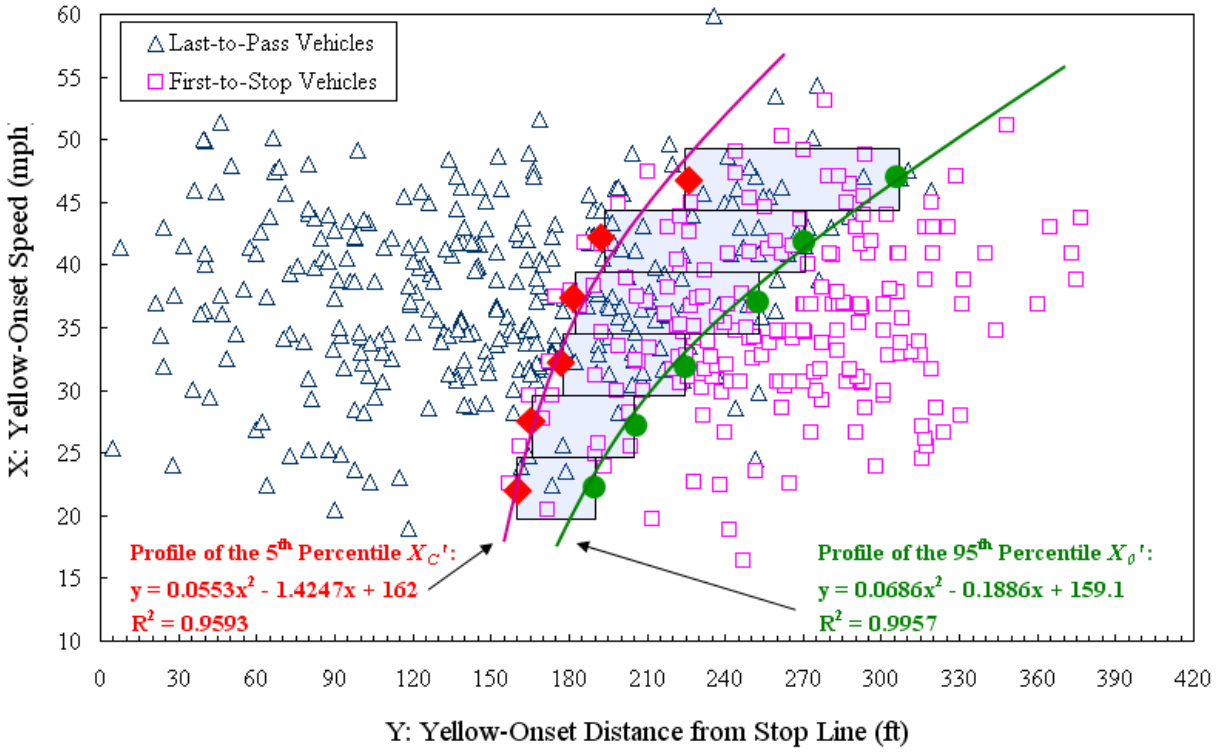

Figure 8. Profiles of the 5th Percentile X_c' and the 95th percentile X_0'

Step 4: with the ground-truth profiles of the 5th percentile X_c' and the 95th percentile X_0', a process of trial-and-fit method is then employed for calibrating the X_0 and X_c models, which is illustrated by Figure 9. The goodness-of-fit analysis shows that the correlation coefficient R^2 is 0.9998 between profiles of X_c' and $X'_{c\text{-}5th}$, while the number is 0.9999 between profiles of X_0' and $X'_{0\text{-}95th}$. Both R^2 values indicate a good fitting. Through the model calibration, appropriate values of $a_{stop}(V_0)$, $a_{pass}(V_0)$, $\delta_{pass}(V_0)$, and $\delta_{stop}(V_0)$ at various speeds are obtained and shown in Table 2. Note that, during the process of calibrating the X_0 model, the "time used by the vehicle to pass the stop line (τ')" is set to 4.23 s, which is equal to the 95th percentile observed value.

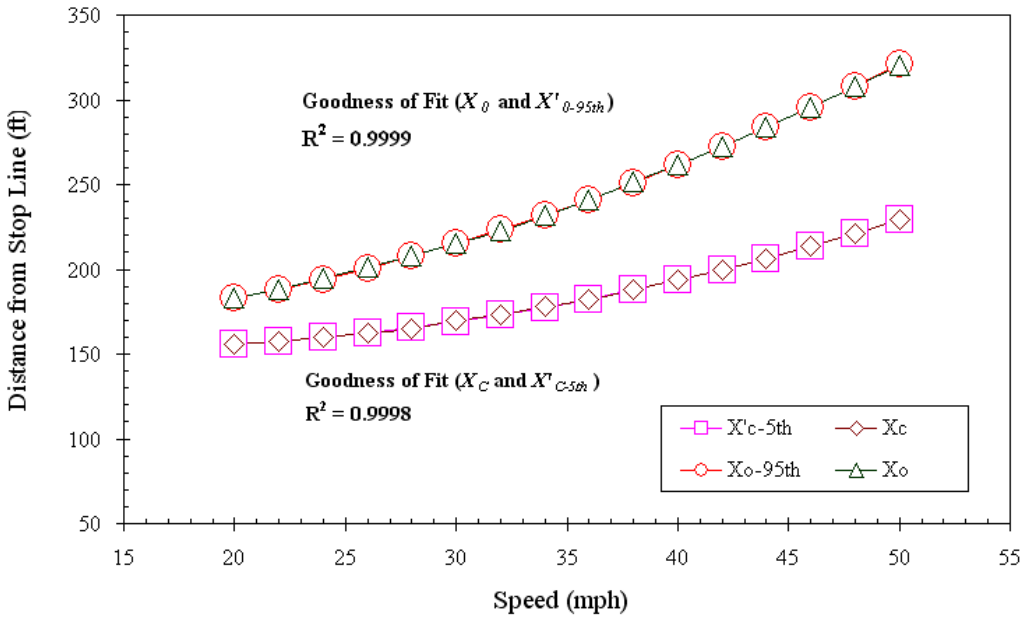

Figure 9. Process of the Model Calibration (Based on Ground-truth Data Set 2)

Table 2. Calibrated Values of Contributing Factors (Based on Ground-truth Data Set 2)

V_0 (mph)	τ' (s)	$\delta_{stop}(V_0)$ (s)	$a_{stop}(V_0)$ (ft/s^2)	$\delta_{pass}(V_0)$ (s)	$a_{pass}(V_0)$ (ft/s^2)	X_c (ft)	X_c' (ft)	X_0 (ft)	X_0' (ft)
20	4.23	0.65	-3.15	0.495	8.45	156	156	183	183
22	4.23	0.645	-3.82	0.47	7.34	157	157	188	188
24	4.23	0.64	-4.51	0.445	6.34	160	160	194	194
26	4.23	0.635	-5.25	0.42	5.46	163	162	201	201
28	4.23	0.63	-6.05	0.395	4.67	165	165	208	208
30	4.23	0.625	-6.82	0.37	3.88	169	169	215	215
32	4.23	0.62	-7.63	0.345	3.23	173	173	223	223
34	4.23	0.615	-8.44	0.32	2.78	178	177	232	232
36	4.23	0.61	-9.27	0.295	2.32	183	182	241	241
38	4.23	0.605	-10.06	0.27	1.98	188	188	251	251
40	4.23	0.6	-10.87	0.245	1.67	194	193	261	261
42	4.23	0.595	-11.65	0.22	1.43	200	200	272	272
44	4.23	0.59	-12.38	0.195	1.31	206	206	284	284
46	4.23	0.585	-13.08	0.12	1.21	213	213	296	296
48	4.23	0.58	-13.76	0.05	1.13	221	221	308	308
50	4.23	0.575	-14.36	0.02	1.09	229	229	320	321

APPLICATIONS OF THE MODEL

Development of the DZ Lookup Charts

Based on the calibrated contributing factors, a dilemma zone lookup chart can be developed. It identifies whether the RZ or the OZ exists, and what the location and length of the dilemma zone

are, for a specific speed and under a certain yellow duration. Figure 10 and Figure 11 illustrate the dilemma zone lookup charts developed based on factor values in Table 1 and Table 2, respectively. The feasibility of placing those X_0 profiles together is based on the research result that change of the yellow duration does not affect the driving behavior including PRT and acceleration/deceleration (Saito et al., 1990; Olson and Rothery, 1961).

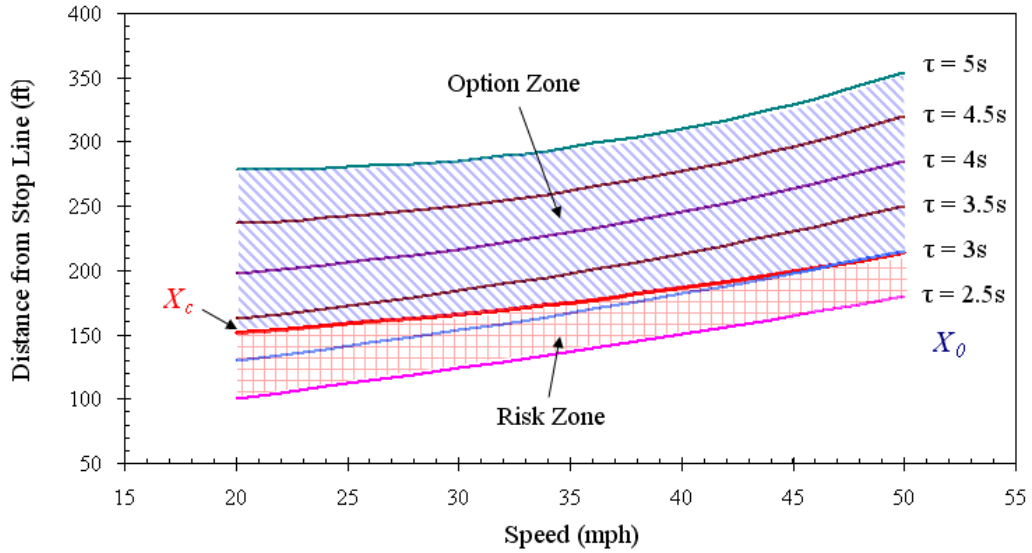

Figure 10. DZ Lookup Chart Developed based on Extreme Driving Behaviors

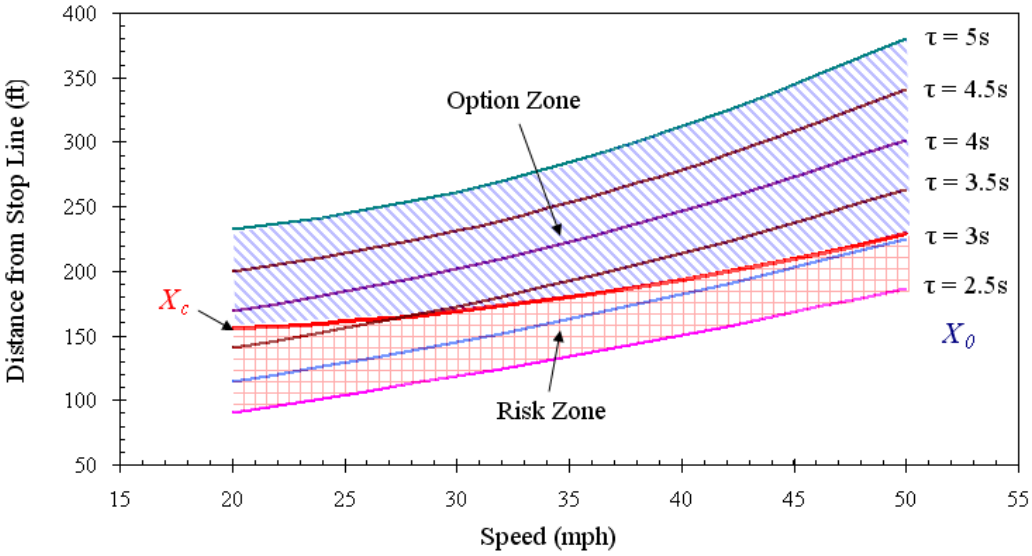

Figure 11. Lookup Chart for 95th Percentile Dilemma Zone

It can be identified from both charts that the length of OZ becomes longer as the yellow duration increases, while the length of RZ becomes shorter as the yellow duration increases. It indicates that prolonging the yellow duration can eliminate the risky zone but will yield a longer OZ. And, it can be also found that higher speed vehicles have a longer OZ and shorter RZ than lower speed vehicles under the same yellow time condition.

The DZ lookup charts describe accurate locations of dynamic dilemma zones, and provide basis for developing corresponding loops layout for dilemma zone protection.

Measurement of Dilemma Hazard

Although the dilemma zone has been recognized as a major cause of some intersection related crashes, its hazard is still hard to be quantitatively measured. However, measurement of dilemma hazard is essential and critical when evaluating the dilemma zone protection performance. Traditionally, it is measured by the average number of vehicles in dilemma zone. Using this measure is based on the assumption that the dilemma zone trapped vehicles have the equal crash probability regardless of their positions. However, it is recognized that the dilemma hazard is not constant, but rather dependent on vehicle's position and speed at the yellow onset (Sharma et al., 2007). Recently, Li and Abbas (2009) proposed a dilemma hazard model and used Monte-Carlo simulation to establish the relationship between a trapped vehicles dilemma hazard and its time to stop line (TTS).

In the study, a new concept of dilemma conflict potential (DCP) is proposed to measure the dilemma hazard faced by the dilemma zone associated vehicles. The DCP is defined as the probability for a dilemma zone associated vehicle to have potential traffic conflicts. Figure 12 helps understand two possible types of traffic conflicts faced by a target vehicle at the onset of yellow. A rear-end (RE) conflict happens if the leading vehicle stops abruptly as the target vehicle intends to pass. And an intersection-angle (IA) conflict takes place if the leading vehicle chooses to pass as the target vehicle attempts to run red.

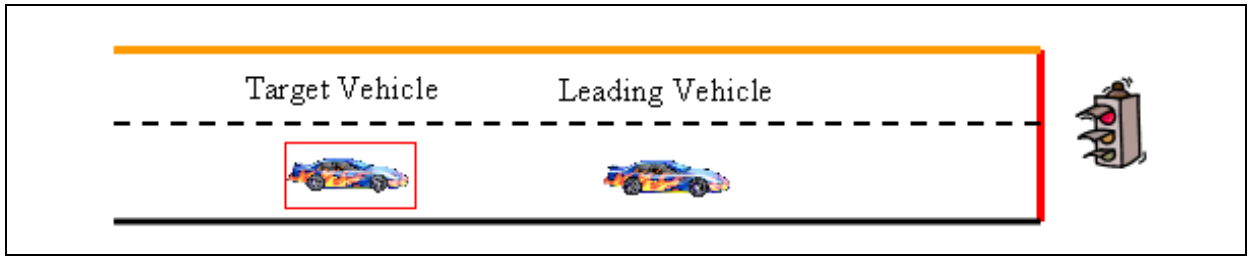

Figure 12. Analysis of Potential Traffic Conflicts

Totally six mutually exclusive, collectively exhaustive scenarios are considered for modeling the DCP for a target vehicle. They cover all possible situations that may lead the target vehicle to a potential dilemma zone related crash (i.e. IA or RE) and they are summarized in Table 3.

Table 3. Possible Dilemma Conflict Scenarios

Scenario	Target Vehicle's Position at the Yellow Onset	Leading Vehicle's Position at the Yellow Onset	DCP
1	in RZ	wherever / none	1
2	in OZ	in OZ	$DCP_{S2}(RE)+DCP_{S2}(IA)$
3	in OZ	in DZ	$DCP_{S3}(RE)+DCP_{S3}(IA)$
4	in OZ	in neither zone/ none	$DCP_{S4}(IA)$
5	in neither zone	in DZ	$DCP_{S5}(RE)$
6	in neither zone	in OZ	$DCP_{S6}(RE)$

Where, $DCP_{Si}(RE)$ is the rear-end DCP for the target vehicle in Scenario i, and $DCP_{Si}(IA)$ is the intersection-angle DCP for the target vehicle in Scenario i. The detailed modeling of the rear-end and intersection-angle DCPs in different scenarios is represented by the following equations.

$$DCP_{S2}(RE) = P_{Tgt}(Pass) \cdot [P_{Ld}(Stop) \cdot P_{Ld}(SA \mid Stop)] \tag{9}$$

$$DCP_{S2}(IA) = [P_{Tgt}(Pass) \cdot P_{Tgt}(RR \mid Pass)] \cdot P_{Ld}(Pass) \tag{10}$$

$$DCP_{S3}(RE) = P_{Tgt}(Pass) \cdot P_{Ld}(Stop) \tag{11}$$

$$DCP_{S3}(IA) = [P_{Tgt}(Pass) \cdot P_{Tgt}(RR \mid Pass)] \cdot P_{Ld}(Pass) \tag{12}$$

$$DCP_{S4}(IA) = P_{Tgt}(Pass) \cdot P_{Tgt}(RR \mid Pass) \tag{13}$$

$$DCP_{S5}(RE) = P_{Tgt}(Pass) \cdot P_{Ld}(Stop) \tag{14}$$

$$DCP_{S6}(RE) = P_{Tgt}(Pass) \cdot [P_{Ld}(Stop) \cdot P_{Ld}(SA \mid Stop)] \tag{15}$$

$$P_{Ld}(SA \mid Stop) = \frac{Noz(SA)}{Noz(Stop)} \tag{16}$$

$$P_{Tgt}(RR \mid Pass) = \frac{Noz(RR)}{Noz(Pass)} \tag{17}$$

Where,

$P_{Tgt}(Pass)$ = the target vehicle's yellow passing probability;

$P_{Ld}(Stop)$ = the leading vehicle's yellow stopping probability;

$P_{Ld}(SA \mid Stop)$ = the conditional probability for the leading vehicle to stop abruptly given it chooses to stop during the yellow interval;

$P_{Tgt}(RR \mid Pass)$ = the conditional probability for the target vehicle to run red given it chooses to pass during the yellow interval;

$P_{Ld}(Pass)$ = the leading vehicle's yellow passing probability;

$Noz(SA)$ = the number of vehicles in OZ at the yellow onset stopping abruptly;

$Noz(Stop)$ = the number of vehicles in OZ at the yellow onset choosing to stop;

$Noz(RR)$ = the number of vehicles in OZ at the yellow onset running red;

$Noz(Pass)$ = the number of vehicles in OZ at the yellow onset choosing to pass.

The stopping and passing probability of either the target or the leading vehicle can be obtained by having it TTS information, when the curve of stopping probability verses TTS is developed from the observed trajectory data using the probit regression method (Sheffi and Mahmassani, 1981), an example of which is illustrated by Figure 13. And, the number of vehicles stopping abruptly or running red can also be obtained from the trajectory data.

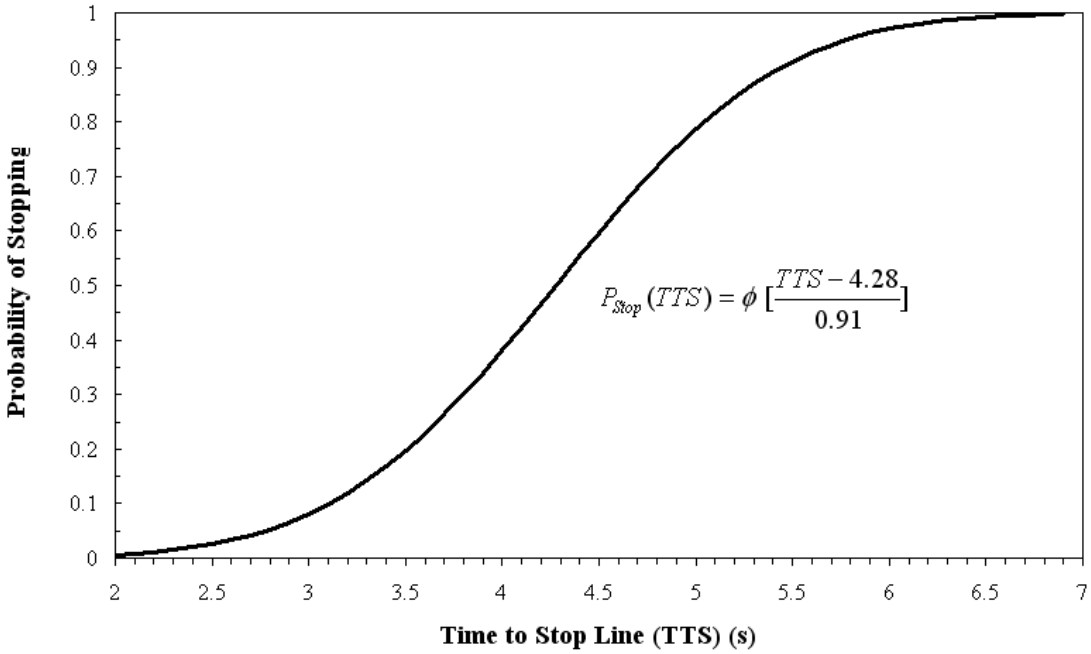

Figure 13. Probability of Stopping (Developped from the Observed Trajectory Data)

The measurement of dilemma hazard for a specific intersection approach consists of the follow steps:

First, obtain the dilemma zone position (whether in RZ, OZ or neither zone) for each vehicle traveling on the approach at the yellow onset by using the DZ lookup chart.

Second, each vehicle will be assumed as a target vehicle and be checked if it pertains to one the six DCP scenarios (Table 3). If yes, calculate the DCP of the corresponding scenario for this vehicle. Otherwise, the DCP for this vehicle is 0.

Third, sum up the DCP of each vehicle for each cycle, and the average DCP per cycle is the quantitative measurement of the dilemma hazard for the intersection approach. It physically represents the potential number of traffic conflicts per cycle for this particular approach.

Proposing and modeling the concept of DCP enable the quantitative measurement of dilemma hazard with respect to the vehicles' yellow-onset position and speed. It provides a measurable index for evaluating the safety performance when developing the strategy of loops layout for dilemma zone protection.

CONCLUSION

In this study, dilemma zone is better understood and its concept is better refined. The results prove that the proposed dilemma zone model is capable of characterizing the dynamics of dilemma zones. And, the extraction of accurate trajectory data enables revealing the inherence pertaining to the dilemma zone dynamics. Moreover, performing statistical analysis on the yellow-onset trajectories is proved to be one of the best ways for interpreting the dilemma zone dynamics into simple mathematical expressions. It derives two alternative ground-truth data sets for calibrating the dilemma zone model at different levels of driving aggressiveness. As a result, the calibrated model has varying values of contributing factors at different approaching speeds, which well reflects the dynamic driving behaviors.

Significantly, the applications of the dilemma zone model establish solid basis for developing advance loops layout strategy for dilemma zone protection. The dilemma zone lookup charts based on the calibrated dilemma zone models provide a practical tool to check the location and length of a dilemma zone for a specific speed and under a certain yellow duration. The 95th percentile dilemma zone is a useful criterion when developing the protection strategy, because it precludes those five percent extremely aggressive drivers and five percent extremely conservative drivers from the protection, which aims to maintain the operational efficiency while enhancing the safety. The DCP concept defined and modeled in this study enables the quantitative measurement of dilemma hazard with respect to the vehicles' yellow-onset position and speed. It provides a measurable index for evaluating the safety performance of a dilemma zone protection strategy.

The methodology used in this study is capable of satisfying the needs of states in the U.S. for updating their local dilemma zone tables. Issues regarding the development of the optimal dilemma zone protection strategy that balances the safety performance and the operational efficiency will be addressed in future research.

ACKNOWLEDGEMENT

This study is part of the project titled "Characterize Dynamic Dilemma Zone and Minimize its Effect at Signalized Intersections", which is funded by the Ohio Transportation Consortium (OTC). Many thanks to OTC for its support all along the project. The results and ideas presented in the paper represent the author's point of views only.

REFERENCES

Chang, G., and Liu, Y. (2006). "Interrelations Between Crash Rates, Signal Yellow Times, and Vehicle Performance Characteristics: Phase II." *Report MD-06-SP508B4B*, Maryland State Highway Administration, MD.

Federal Highway Administration (FHWA) (2006). *Traffic detector handbook 3rd Edition*, Federal Highway Administration.

Gates, T.J., Noyce, D.A., Laracuente,L., and Nordheim, E.V. (2007). "Analysis of Driver Behavior in Dilemma Zones at Signalized Intersections" *Transportation Research Record No. 2030*, Transportation Research Board of the National Academies, Washington, D.C. 29-39.

Gazis, D., Herman, R., and Maradudin, A. (1960). "The problem of the amber signal light in traffic flow." *Operations Research*, 8(1), 112-132.

Institute of Transportation Engineers (ITE) (1982). *Transportation and Traffic Engineering Handbook*, Institute of Transportation Engineers, Prentice Hall.

Institute of Transportation Engineers (ITE) (1999). *Traffic Engineering Handbook*, Institute of Transportation Engineers, Prentice Hall.

Koll, H., Bader, M., Axhausen, K.W. (2004). "Driver's behavior during flashing green before amber: a comparative study." *Accident Analysis and Prevention*, 36(2), 273-280.

Li, P. and Abbas, M.M. (2009). "Optimal Advance Detectors Design for the Multi-detector Green Extension System at High-Speed Signalized Intersections." *TRB 2009 Annual Meeting CD-ROM*, Washington DC.

Moon, Y., and Coleman III, F. (2002). "Dynamic dilemma zone based on driver behavior and car-following model at highway-rail intersections," *Transportation Research – Part B,* 37(4), 323-344.

Moon, Y., Lee, J., Park, Y. (2003). "System Integration and Field Tests for Developing In-Vehicle Dilemma Zone Warning System" *Transportation Research Record No. 1826*, Transportation Research Board of the National Academies, Washington, D.C., 53-59.

Olson, P. and Rothery, R. (1961). "Driver Response to the Amber Phase of Traffic Signals," Operations Research, 9(5), 650-663.

Pant, P. D., Cheng, Y., Rajagopal, A., Kashayi, N. (2005). "Field Testing and Implementation of Dilemma Zone Protection and Signal Coordination at Closely-spaced High Speed Intersections." Report FHWA/OH-2005/006, Ohio Department of Transportation, OH.

Saito, T., Ooyama, N., Sigeta, K. (1990). "Dilemma and Option Zones, the Problem and Countermeasures-characteristics of Zones, and a New Strategy of Signal Control for Minimizing Zones." *Proceedings of the Third International Conference on Road Traffic Control*, London, 137-141.

Sharma A., Bullock D. M., and Peeta, S. (2007). "Recasting Dilemma Zone Design as a Marginal Cost-Benefits Problem." *Transportation Research Record No.* 2035, Transportation Research Board of the National Academies, Washington, D.C., 88-96.

Sheffi, Y. and Mahmassani, H. (1981). "A Model of Driver Behavior at High Speed Signalized Intersections." *Transportation Science*, 15(1), 50-61.

Wei, H., Meyer, E., Lee, J., Feng, C.E. (2005). "Video-Capture-Based Approach to Extract Multiple Vehicular Trajectory Data for Traffic Modeling," *ASCE Journal of Transportation Engineering*, 131(7), 496-505.